Cell Reports, Volume *39*

Supplemental information

FMRP regulates $GABA_A$ receptor channel activity to control signal integration in hippocampal granule cells

Pan-Yue Deng, Ajeet Kumar, Valeria Cavalli, and Vitaly A. Klyachko

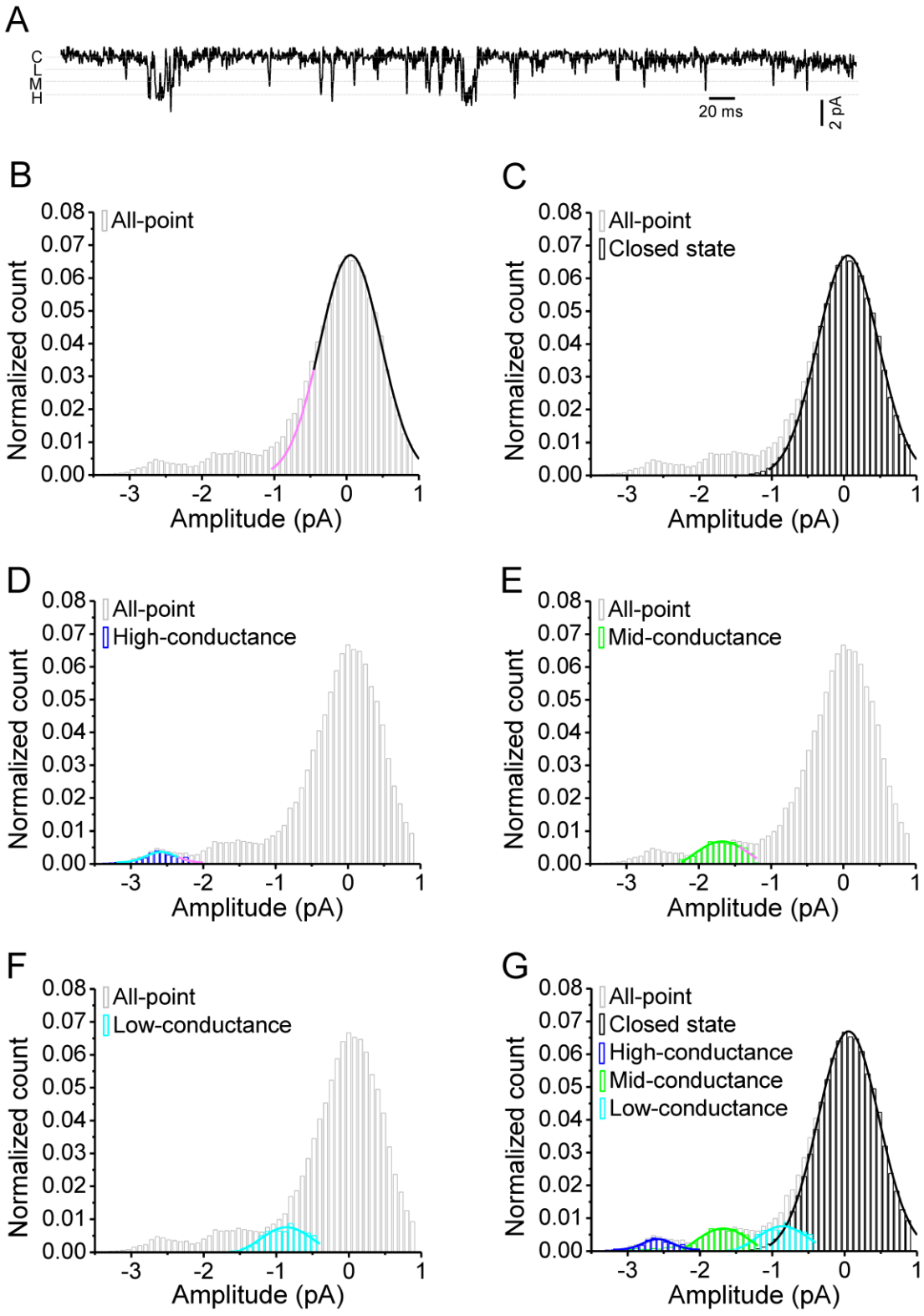

Figure S1. Gaussian fit with subtraction method to isolate 3 conductance states of $GABA_AR$ (related to Figures 1 and 2).

(A) For demonstration purpose, a trace with more high-conductance openings was used. Lines C, L, M and H denote the closed, low-, mid- and high-conductance states, respectively. Initially, we visually identified the C, L, M and H

lines that were used in the first round Gaussian fits. The midpoint values between two neighboring lines were set to be the cutoff points between states. Gaussian fits were performed from both right and left sides of the all-point distribution (right, closed state; and left, high-conductance state) toward the middle (low- and mid-conductance states).

(B, C) First, we plotted the all-point distribution bar graph (normalized to the total number of data points) and fit the closed state by Gaussian function using the bar data right of cutoff point between closed and low-conductance states (black curve of Gaussian fit in B), then extrapolated the fit toward the open direction (pink curve in B). Next, we subtracted the closed state bars (Gaussian fit in C, black curve) from the all point bars. Subsequently, the difference from the subtraction was used for fitting low-conductance state bars. The center value from Gaussian fit of closed state was used to update the C value of the visually defined one in the beginning. The updated C value was then used subsequently for the 2nd round Gaussian fit.

(D) The same fit process as that of the closed state in (B and C), but toward the opposite direction, ie, fit the bars left of the cutoff point between high- and mid-conductance states. Like in (B and C), we performed Gaussian fit and subtraction, and updated H value with the one from Gaussian fit of the high conductance state.

(E, F) After two fits (ie, closed and high-conductance states) and subtractions above, the remaining bars were those of mid- and low-conductance states. We then used the same process to perform the fit for the remaining 2 states, and updated M and L values from corresponding fits.

(G) We used the updated C, L, M and H values to do Gaussian fit with subtraction one more round and again updated C, L, M, and H values from the new fittings. The corresponding single channel currents of 3 open states were the difference between final L/M/H and C values. Open probability was evaluated from area under Gaussian fits (separating neighboring states by cutoff points, which were defined by the midpoint values between neighboring states). The cutoff points were also used to estimate closed and open dwell time.

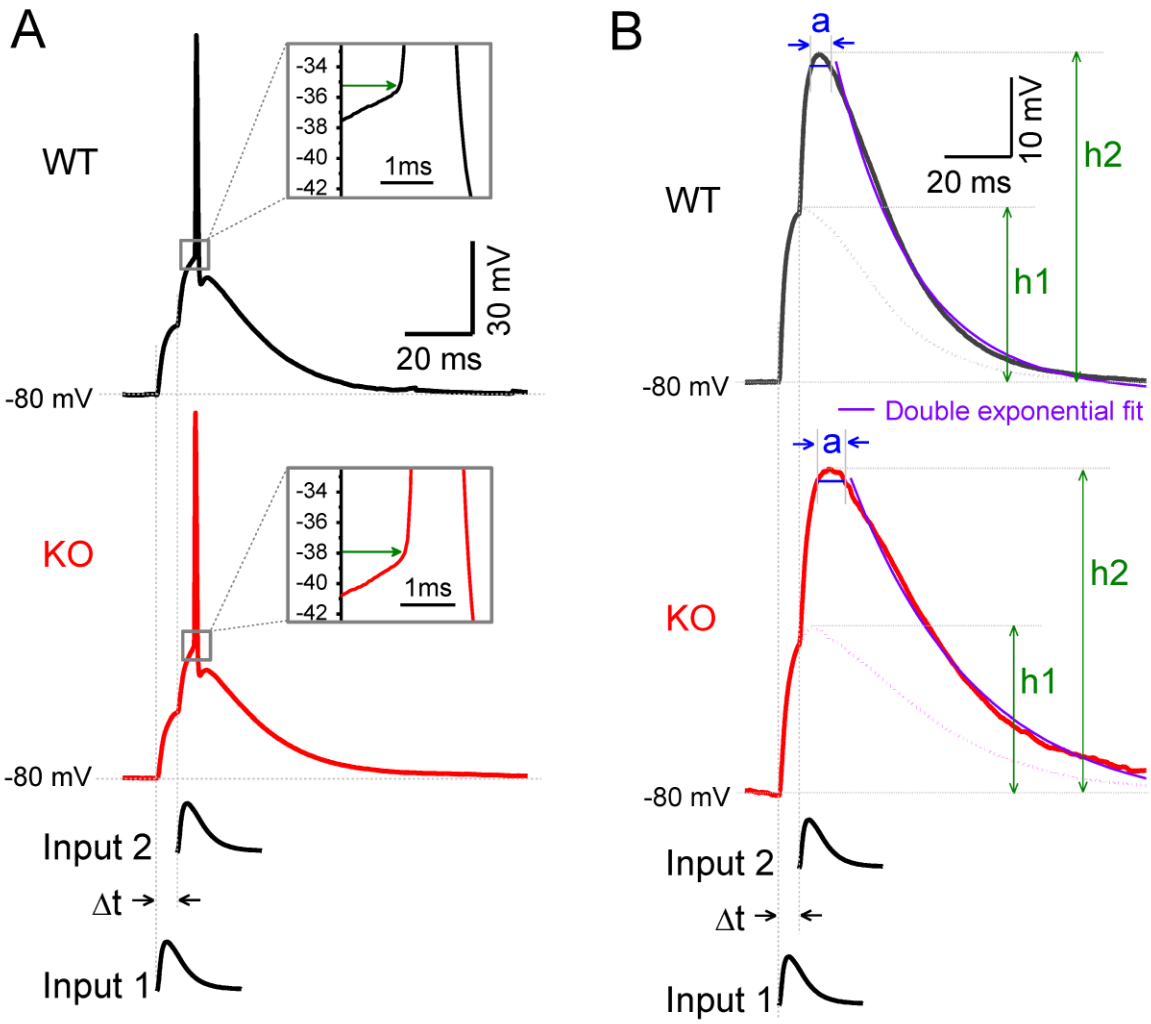

Figure S2. Determination of AP threshold and excitatory potential parameters in GCs (related to Figure 4).

(A) Measurement of AP threshold when EPSC-like currents (low panel, Inputs 1 and 2 with interval Δt) successfully evoked an AP. Note the decreased AP threshold in KO GCs (green arrows in *inserts*).

(B) Measurement of excitatory potential summation ratio (*h2*/*h1*), top width (*a*) and decay time when EPSC-like currents failed to evoke an AP. excitatory potential top width was defined as the width at 97.5% level of h2, because all APs were triggered within this time window in coincidence detection experiments. Note, when only 1-peak excitatory potential occurred in response to stimuli with short intervals ($\Delta t \leq 10$ ms), *h1* was averaged from the first peak of 2-peak excitatory potential of the same trials, as shown in dotted curves.

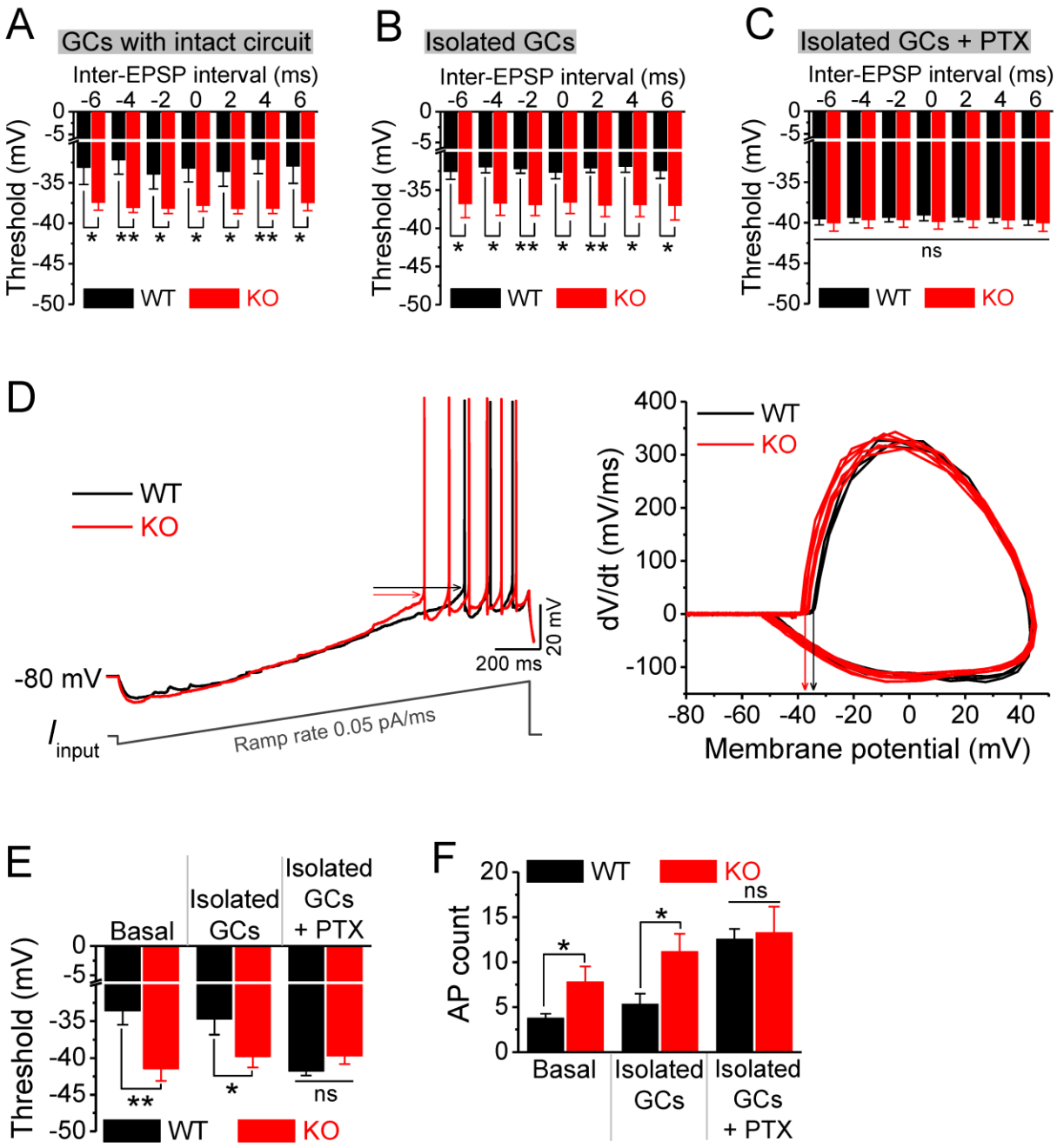

Figure S3. GABA$_A$R dysfunction drives GC hyperexcitability (related to Figure 4).

(A) AP voltage threshold was measured in the coincidence detection experiments when an AP successfully evoked by EPSC-like currents. Loss of FMRP significantly decreased AP threshold. Note that threshold of APs firing at inter-stimulus intervals beyond ±6 ms are not shown due to too few APs fired.

(B) The same as in (A), but recorded from the pharmacologically isolated GCs. Note that the differences in AP threshold between WT and KO neurons remain similar to those observed in (A).

(C) The same as in (B), but in the presence of picrotoxin (PTX, 100 μM) recorded from the pharmacologically isolated GCs.

(D) To further confirm the increased excitability of KO GCs, we employed a ramp protocol (Left, lower) to evoke APs, and examined the AP threshold, as well as the number of AP fired during the ramp. Sample traces showing ramp current-evoked APs (Left, upper) and their phase plots (Right). Arrows (Left and Right) show the difference in threshold level between genotypes (WT in black, KO in red).

(E) AP threshold of GCs with an intact circuit (basal), pharmacologically isolated GCs, and pharmacologically isolated GCs in presence of picrotoxin (PTX) in the ramp protocol-evoked APs.

(F) The same as in (E), but for the number of APs fired during the ramp.

*, $p < 0.05$; **, $p < 0.01$; ns, not significant.

The statistical data are listed in Table S1.

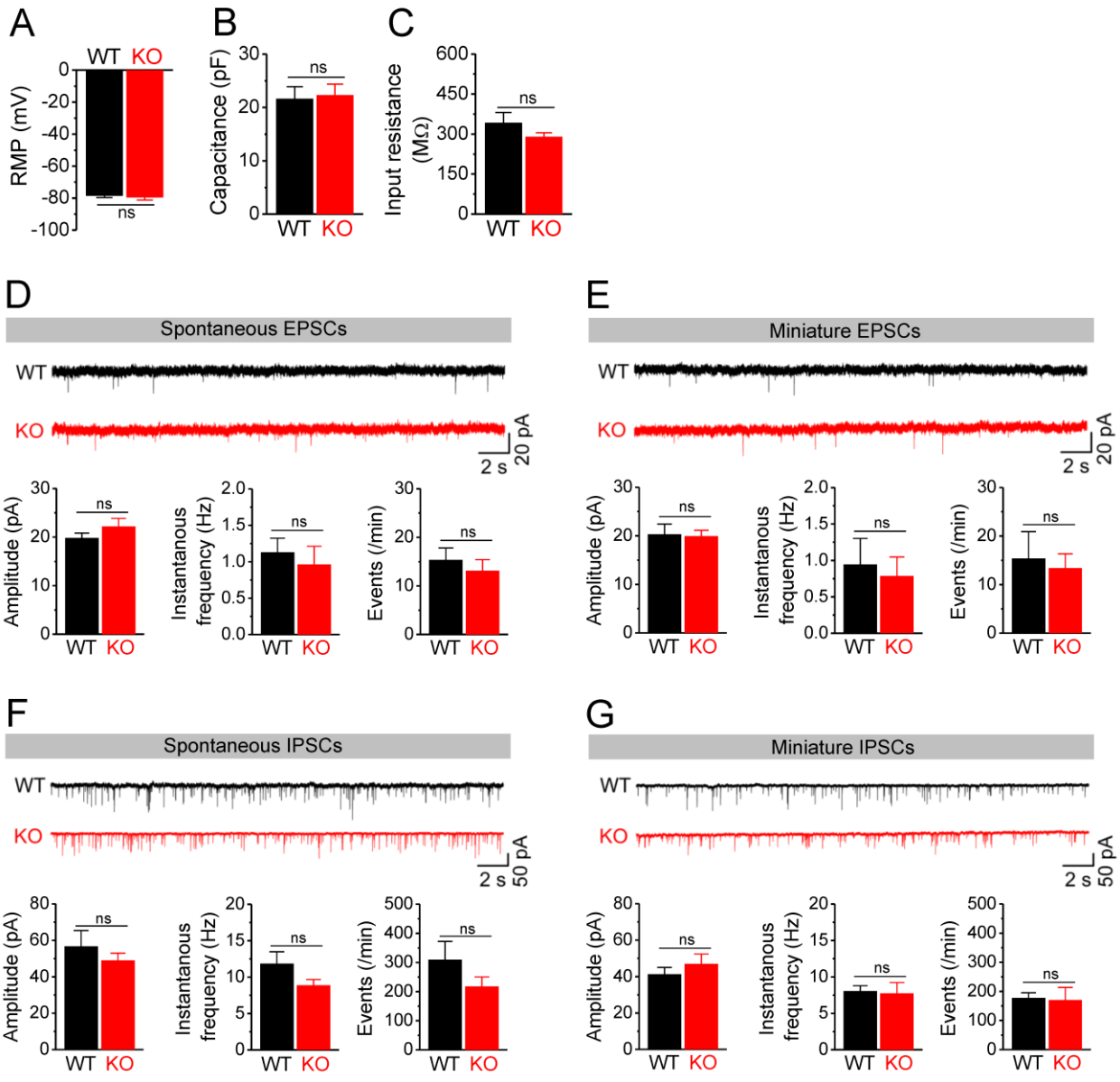

Figure S4. Passive membrane properties and basal inputs were not affected in *Fmr1* KO GCs (related to Figure 4)

(A,B,C) Loss of FMRP did not alter the resting membrane potential (RMP) (A), membrane capacitance (B) and input resistance (C) in GCs.

(D) Sample traces of spontaneous excitatory postsynaptic currents (EPSCs, upper panel). Amplitude (lower panel, left), instantaneous frequency (lower panel, middle) and averaged event count (lower panel, right) of spontaneous EPSCs. Note that loss of FMRP did not change amplitude and frequency of spontaneous EPSCs.

(E) The same as in (D), but for miniature EPSCs (ie, EPSCs recorded in the presence of 1 μM tetrodotoxin).

(F) The same as in (D), but for spontaneous inhibitory postsynaptic currents (IPSCs). IPSCs appear as down-going events due to high chloride internal solution used.

(G) The same as in (E), but for miniature IPSCs (ie, IPSCs recorded in the presence of 1 μM tetrodotoxin).

*, $p < 0.05$; **, $p < 0.01$; ns, not significant.

The statistical data are listed in Table S1.